Water Practice & Technology

 Water Practice & Technology Vol 18 No 5, 1086 doi: 10.2166/wpt.2023.067

Impact of land-use/cover change on water quality in the Mindu Dam drainage, Tanzania

Josephine John Gobry[a,b,*], Sekela Simon Twisa[b], Faustin Ngassapa[a] and Kessy F. Kilulya[a]

[a] Department of Chemistry, College of Natural and Applied Science, University of Dar es Salaam, P. O. Box 35061, Dar es Salaam, Tanzania
[b] Water Institute, P.O. Box 35059, Dar es Salaam, Tanzania
*Corresponding author. E-mail: jgobry@yahoo.co.uk

ABSTRACT

Water pollution caused by land-use/cover change is one of the most pressing problems facing both industrialized and developing countries. Freshwater quality deterioration suggests the collective outcomes of natural courses and alterations in land-use/cover. Understanding the correlation among land-use/cover and water quality parameters is vital for future water quality management. In this work, land-use/cover pattern and its effect on water quality in the Mindu Dam drainage area were analysed using Remote Sensing (RS) and Geographical Information System (GIS) techniques together with cellular automata–Markov model. The land-use/cover images between 1990 and 2020 were used to assess historical and spatial change of land-use/cover change, and projected for 2030 and 2040. We discovered that the dynamics of land use and land cover during the study period were significant. A strong correlation was revealed between changes in the land-use/cover and water quality parameters. Furthermore, a strong correlation exists between cultivated land and measured nutrient (nitrate and phosphate) and chlorophyll-a concentration. The natural vegetation buffer around Mindu Dam should be sufficient to prevent long-term water quality degradation from agricultural runoff in order to manage water quality sustainably. Therefore, land-use/cover management practices must be considered for sustainable resource management and water quality monitoring.

Key words: Geographical Information System, land-use/cover, Mindu Dam, remote sensing, water quality

HIGHLIGHTS

- Land use land cover change.
- Impact of land-use/cover change on water quality.
- Projection of land-use/cover change.
- Water quality sustainability.
- Effect of anthropogenic activities on land cover change.

INTRODUCTION

Land use/cover change is rapidly increasing and has adverse effects and implications at local, regional and global environmental scales (Mzuza *et al.* 2019). In developing countries, the rapid land-use/cover change affects resources such as forests, water quality and quantity, land, soil and vegetation (Twisa & Buchroithner 2019). Increased anthropogenic activities, urbanization, land demand and changing technologies cause land-use/cover change worldwide (Panwar & Malik 2017). Population growth and land development trigger land-use/cover changes, mainly through converting forests into built-up and agricultural land (Dube *et al.* 2014). Further, the struggles to feed the earth's population increase the demand for farmland and fertilizer applications (Vitousek *et al.* 2009). This results in severe deterioration of water quality in most freshwater bodies and presents a risk to human health, biodiversity and food productivity (Ramadas & Samantaray 2018).

Several studies have shown a significant correlation between land-use/cover change and parameters of water quality at a catchment scale (Du Plessis *et al.* 2014; Kibena *et al.* 2014; Teixeira *et al.* 2014; Namugize *et al.* 2018). Land use/cover change is of primary concern in understanding the interactions of human activities with global environmental change (Cheruto *et al.* 2016). It is a fundamental component in modern strategies for managing and monitoring natural resources (Kumari *et al.* 2014) while assessing environmental change at various spatial-temporal scales (Lambin 1997). Water pollution caused by land-use/cover is one of the most pressing concerns facing the world in developed and developing countries (Chaudhry & Malik 2017). Deterioration of freshwater quality suggests the collective outcomes of natural courses and the changes of land-use/cover (Kazi *et al.* 2009).

Land use/cover change results in soil erosion and sedimentation, seriously affecting water quality of small freshwater reservoirs, such as Mindu Dam (Natkhin *et al.* 2015). Understanding the correlation between land-use/cover and water quality parameters is vital for future water quality management (Rajib *et al.* 2016). Viewing the earth from space allows one to study the impact of land-use/cover change on water quality (Cheruto *et al.* 2016; Yang *et al.* 2022).

Several researchers have used techniques such as geospatial modelling, regression modelling and time series analysis to identify the spatial–temporal relationships between water quality changes and different anthropogenic activities (Panwar & Malik 2017; Sagan *et al.* 2020; Tahiru *et al.* 2020). Furthermore, various models have been established to forecast and simulate LULC change, including artificial neural networks, statistical analysis, cellular automata (CA) and Markov chain (Subedi *et al.* 2013). Several studies indicate that combining CA and the Markov model has advantages in studying land use changes (Palinkas *et al.* 2015). When combined with Remote Sensing (RS) and Geographical Information System (GIS), the CA–Markov model becomes a powerful tool for simulating spatial LULC change (Li & Reynolds 1997; Myint & Wang 2006; Guan *et al.* 2011; Riccioli *et al.* 2013; Roose & Hietala 2018). Hence, this study used RS and GIS techniques to analyse and predict land-use/cover patterns around the Mindu Dam catchment area and their effects on water quality. The findings will help water resource managers and decision-makers to take adaptive measures to ensure sustainable water quality development. Furthermore, they will provide the basic scientific knowledge to aid decision-making and future environmental protection in the area.

MATERIALS AND METHODS

Study area

The study was conducted in the Mindu Dam and its surrounds, which are situated at 6.82°S and 37.66°E in the Morogoro region (Figure 1). The Mindu Dam catchment is 303 km^2. The dam collects water from the Mzinga,

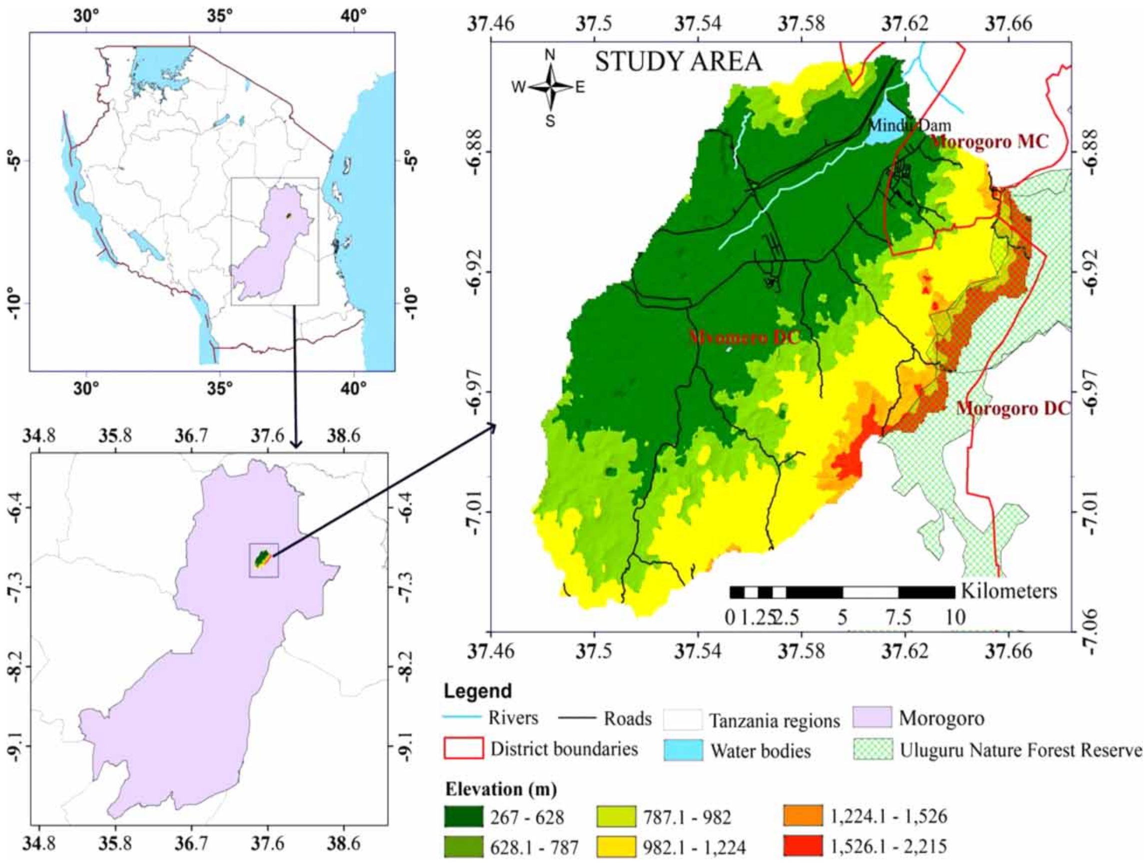

Figure 1 | The study area of Mindu Dam drainage.

Lukulunge, Mugera and Mlali tributaries of the Ngerengere River and the Uluguru mountain ranges. Bimodal rainfall pattern characterizes the catchment, the long rains (March, April and May) and the short rains (September, October and November). The annual rainfall in the area is between 800 and 1,500 mm, with an average of 890 mm. In total, 80% of the freshwater used in Morogoro's urban and peri-urban areas comes from the Mindu Dam (Ngonyani & Nkotagu Hudson 2007; Mdegela *et al.* 2009).

The Mindu Dam is the main source of freshwater provisions in the municipal and peri-urban communities of Morogoro (Mdegela *et al.* 2009). The main socioeconomic activities in the catchment include crop cultivation, fishing and small-scale mining and settlement development. These anthropogenic pressures result in nutrient enrichment from agricultural runoff and industrial wastewater discharge, affecting water quality (Mdegela *et al.* 2013). Analysing and predicting land-use/cover change around the Mindu Dam is important for natural and socioeconomic development on spatial and temporal scales (Kamusoko *et al.* 2011; Dube *et al.* 2014).

Land use/cover change analysis

Clouds-free Landsat satellite images between 1990 and 2020 were used to evaluate land-use/cover change in the study area (Table 1). The satellite images were accessed from the United States Geological Survey – USGS website (https://glovis.usgs.gov/). The images were classified using the hybrid classification method, which combines both commonly used supervised (Maximum Likelihood Classification – MLC) and unsupervised (Iterative Self-Organizing Data Analysis – ISODATA) methods (Sun *et al.* 2013; Li *et al.* 2014; Kumar *et al.* 2020; Rozario & Gomes 2021). The classification was initially carried out using the ISODATA method. In this case, a maximum of 32 land-use/cover classes were formulated. The formulated classes were visually interpreted based on ground truthing data, base map and Google Earth images. Similar classes were combined and recorded into major land-use/cover classes established during ground truthing. Then, the ISODATA output was included in MLC. In this case, a classification scheme major from CCI Global was adopted. The major land cover classes included in the MLC were; forest, woodland, bushland, grassland, waterbodies, cultivated land, built-up areas and bare land. The accuracy was evaluated with both visual judgement and confusion matrix. Change detection was conducted through overlay (intersection) techniques according to Kashaigili & Majaliwa (2010).

Table 1 | Detailed data on the Landsat images used in this study

Year	Satellite	Sensor	Path/Row	Acquisition date	Cloud cover
1990	Landsat 5	TM(SAM)	167/65	15 July 1990	1%
2000	Landsat 7	ETM(SAM)	167/65	07 July 2000	2%
2010	Landsat 7	ETM(BUMPER)	167/65	10 July 2010	9%
2020	Landsat 8	OLI	167/65	16 September 2017	2.42%

Land use/cover prediction using CA–Markov

To better simulate temporal and spatial patterns of land-use/cover changes in quantity and space, the combination of cellular automata and Markov Chain (CA–Markov) was developed using IDRISI Selva 17.0 software. It involved two main stages: calculating conversion probability using Markov chain analysis and spatial specification of land-use/cover coverage simulated based on CA spatial operator and multi-criteria evaluation (MCE).

The mathematical expression of the Markov model is presented in Equation (1):

$$S(t+1) = P_{ij} * S(t) \tag{1}$$

where $S(t+1)$ represents the status of LULC at a time $(t+1)$, P_{ij} represents a transitional matrix in Equation (2):

$$P_{ij} = \begin{bmatrix} P_{11} & P_{12} & P_{13} & \dots & P_{1n} \\ P_{21} & P_{22} & P_{23} & \dots & P_{2n} \\ P_{31} & P_{32} & P_{33} & \dots & P_{3n} \\ \dots & \dots & \dots & \dots & \dots \\ P_{n1} & P_{n2} & P_{n3} & \dots & P_{nn} \end{bmatrix} \tag{2}$$

$(0 \leq P_{ij} < 1)$ and $\sum_{j=1}^{n} P_{ij} = 1$. Where $(i, j = 1, 2, \ldots, n)$. i and j are the land uses and P_{ij} represents the transition probability between any pair of land uses. From the matrix, the rows and columns represent historical and current LULC classes, respectively. Furthermore, the CA's mathematical expression is presented in Equation (3):

$$S(t,\ t+1) = f(S(t), N) \tag{3}$$

For model validation, the simulated land-use/cover map for 2020 was compared with the actual satellite-derived land-use/cover map based on the Kappa statistics. Then, the standard Kappa index was used to check whether the model is valid (usually, the Kappa index for an accurate model is >70%). Using the VALIDATE tool, IDRISI gave the Kstandard of 0.80, Kno of 0.84, Klocation of 0.83 and Kstratum of 0.83, all above 0.7.

Determination of water quality

The samples for water quality analysis were collected in triplicate (at surface, 1 and 2 m depth) from well-distributed 30 sampling points within the dam (APHA 2012). The location was recorded using handheld GPS. The water samples for measuring Chl-a were collected in amber bottles, stored in the dark (to prevent photodegradation), frozen at −4 °C and transported to a laboratory until further processing. The integrated sample of 500 mL was prepared, and 200 mL was filtered through glass microfibre filters grade C GF/C 47 mm (Whatman™) filter paper and stored at 4 °C in the dark for Chl-a extraction. Furthermore, water samples were collected for the analysis of temperature, pH, nitrate and phosphorus as per the Standard Methods for the Examination of Water and Wastewater (APHA 2012). Following collection, the samples for nutrient analysis were preserved as per APHA (2012) and transported to the laboratory for analysis. The cadmium reduction method and ascorbic acid methods were used for the analysis of nitrates (NO_3^-) and phosphates (PO_4^{3-}), respectively, with a DR6000 (Hach Spectrophotometer) (APHA 2012). Physicochemical parameters (temperature and pH) were analysed in triplicates onsite by using a portable meter (YSI 556 MPS, USA). The chlorophyll-a concentrations were determined with a spectrophotometer, and pigment extraction was conducted in subdued light to avoid degradation. Pigment extraction from the GF filters was carried out using 90% analytical grade acetone whereby filters were placed in a test tube for extraction using 10 ml acetone overnight. The mixture was macerated at 500 rpm for 1 min at 4 °C. After centrifugation, the supernatant was immediately used for pigment quantification. Absorbance was measured at 400–750 nm using spectrophotometer (UV-1800PC, China).

Water quality variables for the past year (1990–2010) were accessed from the Water Institute (Dar es Salaam).

The linear relationship between land-use/cover variables and water quality parameters

Pearson correlation analysis was performed to determine the correlation between water quality parameters and land-use/cover change for Mindu Dam. In case, the mean change percentage of land use area in the basin between 1990 through 2020 was correlated with corresponding mean water quality values to establish the significance of the relationship between land use and water quality parameters (Palinkas *et al.* 2015; Tahiru *et al.* 2020) using the following equation:

$$r = \frac{\sum (x_i - \bar{x})(y_i - \bar{y})}{\sqrt{\sum (x_i - \bar{x})^2 \sum (y_i - \bar{y})^2}} \tag{4}$$

where r is the correlation coefficient; x_i is the values of the x-variables in a sample; $\bar{x}$ is the mean of the values of the x-variables; y_i is the values of the y-variables in a sample; and $\bar{y}$ is the mean of the values of the y-variables.

The Pearson correlation analyses were performed using XLSTAT. Pearson correlation coefficient 'r' was considered significant at $p < 0.05$.

RESULTS AND DISCUSSION

Land use/cover change pattern

The trend of land-use/cover change from 1990 to 2020 based on eight classes extracted from Mindu Dam drainage is presented in Tables 2 and 3. Additionally, the spatial representation of land-use/cover types from 1990 to 2020 is shown in Figures 2–4. In the year 1990, the pattern of land-use/cover calculated as the percentage of the total area studied was dominated by woodland, covering 40.25% of the total studied area, followed by bushland, forest, cultivated land, grassland, water, built-up area and bare land (Table 2). Moreover, trend changes were

Table 2 | Results of land-use/cover classification for 1990, 2000, 2010 and 2020 images

Year Land use/cover	1990 Ha	1990 %	2000 Ha	2000 %	2010 Ha	2010 %	2020 Ha	2020 %
Forest	4,452	14.93	2,978	9.98	2,046	6.82	1,568	5.25
Woodland	12,011	40.25	8,000	26.81	4,219	14.14	2,614	8.76
Bushland	8,744	29.30	11,646	39.02	9,751	32.68	6,790	22.75
Grassland	597	2.00	1,465	4.91	5,336	17.89	4,944	16.57
Water	233	0.78	224	0.75	226	0.76	226	0.76
Cultivated land	3,700	12.40	5,408	18.12	8,074	27.06	13,303	44.58
Built-up area	79	0.26	93	0.31	124	0.42	204	0.68
Bare land	26	0.09	30	0.10	67	0.22	194	0.65
Total	**29,843**	**100**	**29,843**	**100**	**29,843**	**100**	**29,843**	**100**

Table 3 | Results of the land-use/cover change from 1990 to 2020

Year (change) Land use/cover	1990–2000 Ha	1990–2000 %	2000–2010 Ha	2000–2010 %	2010–2020 Ha	2010–2020 %	1990–2020 Ha	1990–2020 %
Forest	−1,474	−4.95	−932	−3.16	−478	−1.57	−2,884	−9.68
Woodland	−4,011	−13.44	−3,781	−12.67	−1,605	−5.38	−9,397	−31.49
Bushland	2,902	9.72	−1,895	−6.34	−2,961	−9.93	−1,954	−6.55
Grassland	868	2.91	3,871	12.98	−392	−1.32	4,347	14.57
Water	−9	−0.03	2	0.01	0	0	−7	0.02
Cultivated land	1,708	5.72	2,666	8.94	5,229	17.52	9,603	32.18
Built-up area	14	0.05	31	0.11	80	0.26	125	0.42
Bare land	4	0.01	37	0.12	127	0.43	168	0.56

observed for all land-use/cover in 2000, 2010 and 2020, except for water, with the smallest changes. In 2020, the observed land-use/cover pattern was dominated by cultivated land (44.58%) followed by bushland, grassland, woodland, forest, water, built-up area and bare land (Table 2). This might be the result of population growth in the area. An increase in population increases food requirements to sustain livelihoods, resulting in land demand for cultivation. The findings agree with that of Mzuza *et al.* (2019); high population pressure led to increased conversion of forested land to cultivation land.

Furthermore, the pattern of land-use/cover changes during the studied period (1990–2020) indicates a general decrease in woodland, forest, bushland, while an increase was observed on cultivated land, grassland, bare land and built-up area (Table 3). This is probably due to the intensification of human activities on natural resources. The negative annual rate increase change between 1990 and 2020 was detected in woodland, forest and bushland, while positive annual increase change was detected in cultivated land, grassland, built-up area and bare land (Table 4). This shows the transition of natural resources to agricultural activities and human settlements.

Land use/cover transition matrix

Further land-use/cover change analysis was performed by observing the areas changed with their corresponding percentages based on the transition matrix cross-tabulation from 1990 to 2020 (Table 5). This shows a detailed image of the plots of land that were transformed from one class to another. The highest conversion (Table 5) was observed in grassland, as almost 43.15% of the total area was converted to woodland. The rest was converted to bushland (30.83%), forest (12.16%), cultivated land (10.57%) and a total of (0.24%) to water, built-up area and bare land. Most of the forest was converted to woodland (10%), while more significant portion of cultivated land was converted to bushland (39.45%). During the study duration (1990–2020), 91.40% of water remained intact, followed by forest, woodland, bushland, cultivated land, built-up area, bare land and grassland. The remaining

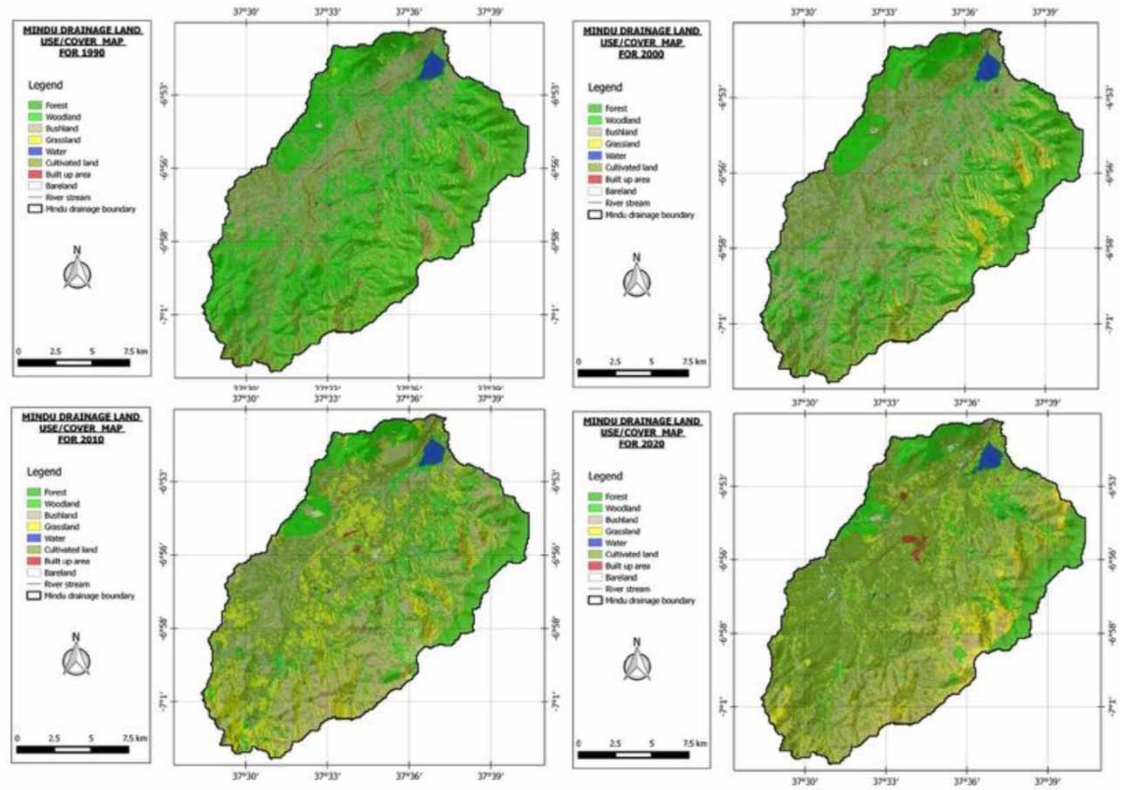

Figure 2 | Land use/cover maps for 1990, 2000, 2010 and 2020. (Data source: USGS, map prepared by authors of this study.)

forest area decreased to 67.06% in the period 2000–2010. Forest loss during this period was likely due to illegal charcoal production and subsistence farming. The efforts to recover the lost forest were observed in 2010–2020, where 75.17% of the forest area remained intact. Although the forest did not change much, almost 24.99% was gained from woodland, followed by bushland 20.18%, grassland (12.16), water (6.05%), bare land (3.48%) and cultivated land (3.24%). The change speed of one land-use/cover between 1990 and 2020 was relatively slow, but the highest conversion was experienced in the grassland, with 10% converted to cultivated land. The transformation was probably due to the higher population. People tend to search for cheaper land for accommodation and farming. The results for the study area from 1990 to 2020 on different classes of land-use/cover shows that woodland and bushland experienced the highest conversions to grassland and cultivated land. Similar trends have been reported by Hassan *et al.* (2016), whereby agricultural increase converted bushland and woodland into cultivated land, and the abandoned former farms became grasslands.

Conditional probability matrix and land-use/cover pattern for predicted land-use/cover

Each pixel conditional probability matrix to belong to a specified class in 2040 from 2020 is expressed in Table 6 and Figure 3. Thus, the transitional probability matrix is presented cartographically in these maps. During 2020 and projected 2040, 13% of bare land remained unchanged, followed by 16% grassland, 27% for both woodland and bushland, 49% for the forest, 50% of built-up area, 51% of cultivated land and 78% of the water. These results indicate that bare land and grassland will be most affected, with the probability that 43% of bare land will be converted to bushland while 59% will be converted to cultivated land. The projection results showed that the built-up area, cultivated land and water would all remain above 50% of their current land-use/cover, while the most significant share for cultivated land will be gained from grassland

The extent of land-use/cover types projected in 2030 and 2040 is shown in Table 7 and predicted maps in Figure 4. Projection of land cover for the study area for 2030 and 2040. Land use/cover of the year 2030 indicated that the area would be covered by cultivated land (46.20%), followed by bushland, grassland, woodland and forest and built-up area, bare land and water. Additionally, the area will be covered by cultivated land (47.80%), grassland, bushland, woodland, forest, built-up area, bare land and water by 2040. Forest, woodland, bushland and water are predicted to experience net losses by 2040, whereas grassland, cultivated land, built-up area and

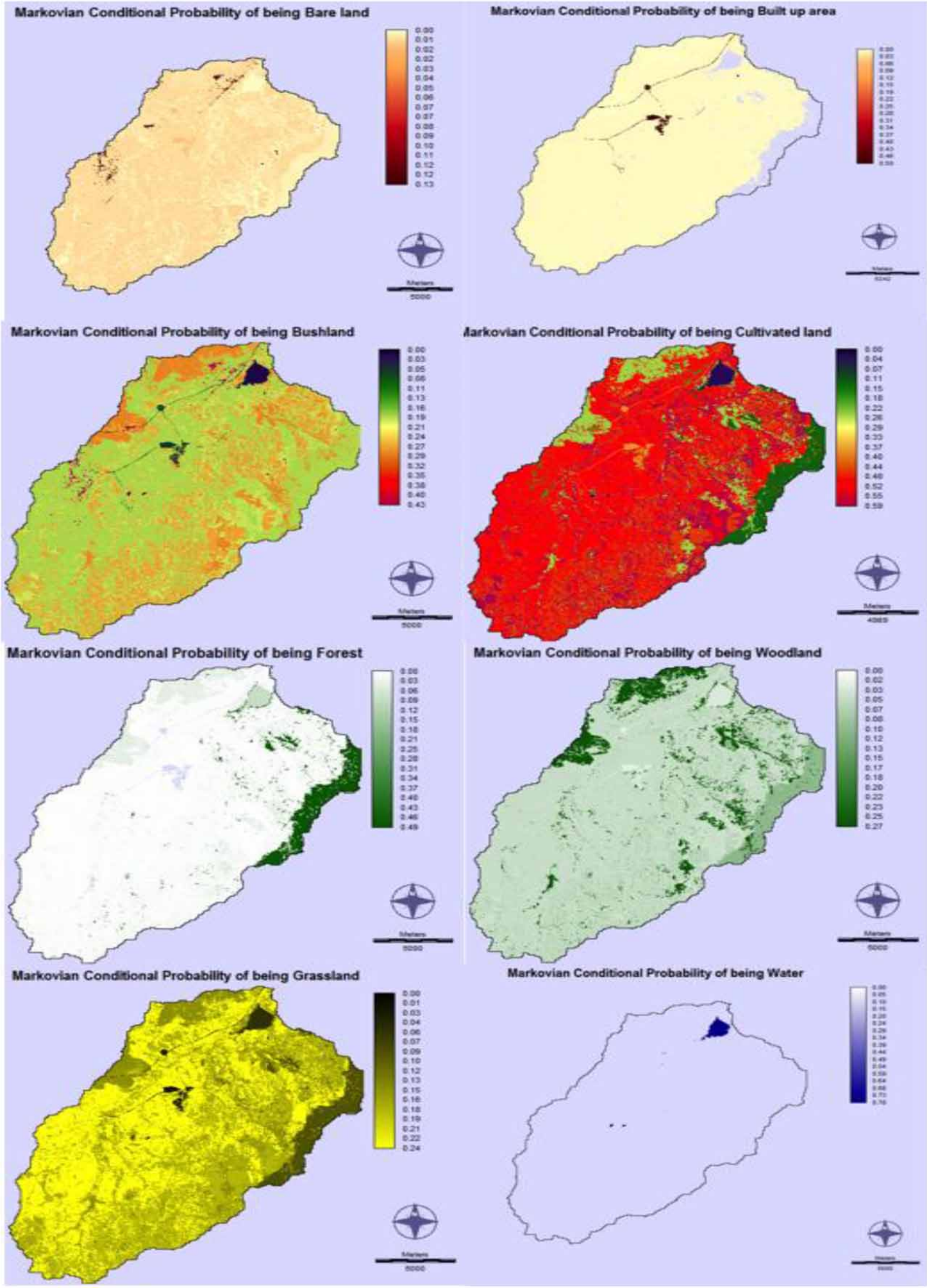

Figure 3 | Markovian conditional probability of individual land-use/cover. (Data source: USGS, map prepared by authors of this study.)

bare land are predicted to experience net gains. The land cover and use are geared at expanding the amount of cultivated land. The increase of cultivation land is expected to be due to the pressure from the growing population that leads to the expansion of land for agricultural activities.

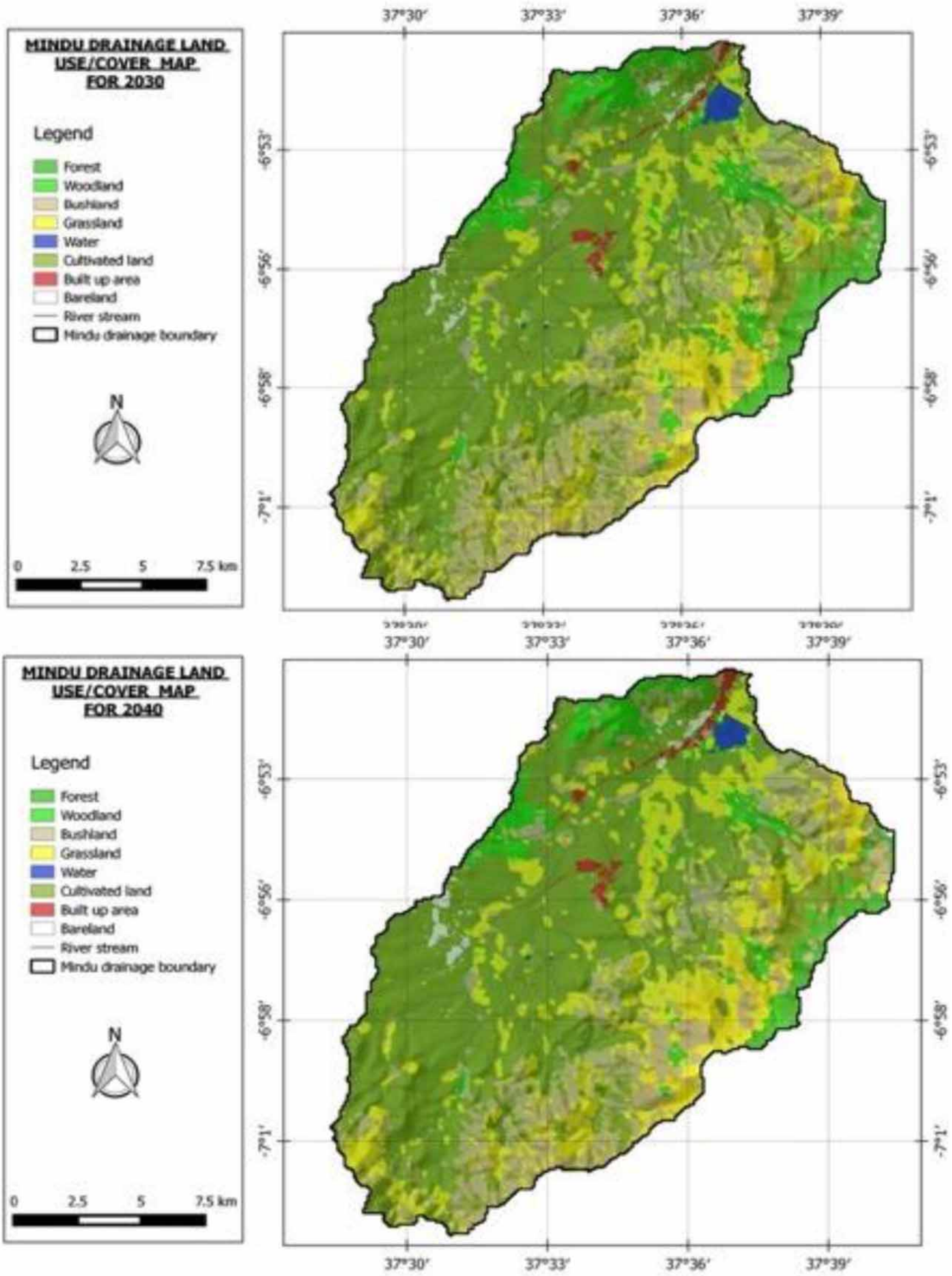

Figure 4 | Projected land-use/cover for the year 2030 and 2040. (Data source: USGS, map prepared by authors of this study.)

Water quality parameters results

The mean chlorophyll-a concentration of 30 samples was (83.277 μg/L) and a relatively high standard deviation (46.30582 μg/L) was recorded, which indicated the spatial variability of chlorophyll-a concentration (Table 8). The highest concentration (140.181 μg/L) was recorded at point S11. The mean concentrations of phosphate, nitrate, pH and temperature were 0.82 ± 1.35 mg/L, 2.63 ± 1.28 mg/L, 7.87 ± 0.35 and 27.96 ± 0.95,

Table 4 | Results of land-use/cover annual rate change

Year Land use/cover	1990–2000 (ha/year)	2000–2010 (ha/year)	2010–2020 (ha/year)	1990–2020 (ha/year)
Forest	−211	−93	−68	−125
Woodland	−573	−378	−229	−409
Bushland	414	−189	−423	−85
Grassland	124	387	−56	189
Water	−1	0	0	0
Cultivated land	244	267	747	418
Built-up area	2	3	11	5
Bare land	1	4	18	7

Table 5 | Transition matrix showing land-use/cover change between 1990 and 2020

		2020							
	Area (ha)	**FR**	**WL**	**BL**	**GL**	**WT**	**CL**	**BLT**	**BL**
1990	FR	1,378	156	16	4	9	4	0	1
	WL	653	1,483	353	53	3	61	4	4
	BL	1,370	3,296	1,412	120	3	577	6	6
	GL	601	2,133	1,524	151	7	522	3	2
	WT	14	3	2	0	207	1	0	0
	CL	431	4,849	5,249	266	4	2,462	36	6
	BLT	0	48	90	0	0	36	30	0
	BL	7	42	99	3	0	38	0	6
	Percentage (%)	**FR**	**WL**	**BL**	**GL**	**WT**	**CL**	**BLT**	**BL**
1990	FR	**88**	10	1	0	1	0	0	0
	WL	24.99	**56.74**	13.49	2.02	0.12	2.34	0.14	0.16
	BL	20.18	48.54	**20.80**	1.77	0.04	8.49	0.08	0.09
	GL	12.16	43.15	30.83	**3.05**	0.14	10.57	0.06	0.04
	WT	6.05	1.51	0.72	0.00	**91.40**	0.32	0.00	0.00
	CL	3.24	36.45	39.45	2.00	0.03	**18.51**	0.27	0.05
	BLT	0.09	23.48	44.22	0.00	0.00	17.52	**14.70**	0.00
	BL	3.48	21.51	50.76	1.48	0.00	19.61	0.09	**3.06**

FR, Forest; WL, Woodland; BSL, Bushland; GL, Grassland; WT, Water; CL, Cultivated land; BLT, Built-up land; BL, Bare land.
Note: The bold numbers on the diagonal show the percentage land use/cover that remained unchanged from 1990 to 2020, while the other numbers show the percentage that are converted from one class to another.

Table 6 | Transitional probability matrix for land use/cover change 2020 to 2040

		2040							
	Percentage Land-use/cover	**FR**	**WL**	**BSL**	**GL**	**WT**	**CL**	**BLT**	**BL**
2020	FR	**49**	10	19	9	0	13	0	0
	WL	4	**27**	29	14	0	25	0	1
	BSL	2	6	**27**	18	0	46	0	1
	GL	0	4	19	**16**	0	59	1	0
	WT	9	3	1	6	**78**	2	0	0
	CL	0	5	18	24	0	**51**	1	1
	BLT	0	2	6	3	0	38	**50**	1
	BA	1	5	43	19	0	19	1	**13**

FR, Forest; WL, Woodland; BSL, Bushland; GL, Grassland; WT, Water; CL, Cultivated land; BLT, Built-up land; BL, Bare land.
Note: Bold numbers on the diagonal represent percentages of Land use/cover that remained unchanged from 2020 to 2040, whereas other numbers represent percentage that had changed from one class to another.

Table 7 | Areas of individual land-use/cover change in the projected years 2030 and 2040

Year / Land use/cover	2030		2040		2020–2030		2030–2040		2020–2040	
	Ha	%	Ha	%	Ha	%	Ha	%	Ha	%
Forest	1,102	3.69	640	2.15	−466	−1.56	−462	−1.55	−928	−3.11
Woodland	2,162	7.25	1,709	5.73	−453	−1.51	−453	−1.52	−906	−3.03
Bushland	6,393	21.37	5,982	20.00	−397	−1.38	−411	−1.38	−808	−2.75
Grassland	5,718	19.17	6,495	21.78	774	2.60	777	2.61	1,551	5.21
Water	189	0.63	153	0.51	−37	−0.12	−35	−0.12	−73	−0.24
Cultivated land	13,778	46.20	14,257	47.80	475	1.62	479	1.61	954	3.23
Built-up area	266	0.89	329	1.10	62	0.21	62	0.21	124	0.42
Bare land	236	0.79	278	0.93	42	0.14	42	0.14	84	0.28
Total	**29,843**	**100**	**29,843**	**100**						

Table 8 | Results and statistics for pH, temperature, chlorophyll-a, phosphate and nitrate as of 2020

Year	Chlorophyll-a (mg/m^3)	Phosphate (mg/L)	Nitrate (mg/L)	pH	Temp (°C)
1990	34.65 ± 1.45[a]	0.09 ± 0.01[a]	0.07 ± 0.01[a]	7.01 ± 0.05[a]	27.01 ± 0.11[a]
2000	46.77 ± 7.82[b]	0.12 ± 0.02[a]	0.91 ± 0.11[a]	7.17 ± 0.13[a]	26.90 ± 0.25[a]
2010	59.20 ± 15.67[c]	0.62 ± 0.01[b]	1.05 ± 0.17[c]	7.27 ± 0.22[b]	27.06 ± 0.24[a]
2020	83.28 ± 46.31[e]	0.82 ± 1.35[c]	2.63 ± 1.28[d]	7.87 ± 0.35[c]	27.96 ± 0.95[b]

Values that do not share the same superscript in the same column are statistically different at $p < 0.05$.

respectively. The high concentration of 7.851 mg/L was measured at sampling point S24 for phosphate and 7.618 mg/L for nitrate at sampling point S30.

Pearson correlation analysis

Table 9 presents the results of correlation analysis between land-use/cover change and the average values of the water quality parameters. The patterns revealed that chlorophyll-a (Chl-a) was significantly and negatively correlated to change in forest, woodland and bushland but positively correlated to change in cultivated land, built-up and bare land. Phosphate (P) significantly and negatively correlated to bushland but positively correlated with change in cultivated land, built-up and bare land. Nitrate (N) was significantly and negatively correlated to change in forest, woodland and bushland but positively correlated with change in grassland, cultivated land, built-up and bare land. pH significantly and negatively correlated to change in forest and woodland but positively correlated with change in cultivated land, built-up and bare land. Similarly, water temperature significantly and negatively correlated to change in forest and woodland but positively correlated with change in cultivated land, built-up and bare land.

Table 9 | Pearson correlation coefficients between land-use/cover change and water quality parameters

Variable	Forest	Woodland	Bushland	Grassland	Cultivated land	Built-up area	Bare land
Chl-a	−0.62*	−0.68*	−0.65*	0.44	0.99**	0.99**	0.96*
P	−0.46	−0.49	−0.62*	0.11	0.95*	0.98**	0.99*
N	−0.69*	−0.77*	−0.62*	0.61*	0.97*	0.95*	0.88*
pH	−0.77*	−0.83*	−0.51	0.57	0.98*	0.95*	0.88*
Temp	−0.90*	−0.91*	−0.24	0.52	0.93*	0.88*	0.77*

*$p < 0.05$; **$p < 0.01$.

The strong correlation between cultivated land and nitrate, phosphate and chlorophyll-a concentration might be due to an increase in agricultural land which intensify the use of chemical fertilizers and pesticides that results in water quality deterioration. These findings are supported by Ranjan & Kumari (2018), that intensive agricultural practices negatively affect water quality. The quality of water is also affected by human interference related to urbanization and land development. The findings of this study reveal that the areas for cultivated land and the built-up area increase all the time, including urbanization and industries, which might have been the leading cause of water quality degradation in the Mindu Dam. The findings agree with that of Azyana *et al.* (2012) that developed lands were the best indicator for predicting water quality degradation. Water resource planning essentially resolves into three issues: the extent of available water resources in terms of quantity and quality, the future requirements of water for various purposes, and how these can be met. This calls for action on what causes land-use/cover change, especially the contribution by human activities and provides a legal framework to guide the activities to ensure sustainable use of available land.

CONCLUSIONS

This study aimed to analyse and predict land-use/cover change and its effects on water quality parameters in Mindu Dam. The study revealed that cultivated land and built-up areas activities are the primary sources of water quality deterioration in the study area. An increase in population and land development creates demand for water resources, increasing stress on the aquatic ecosystem. The buffer of natural vegetation surrounding Mindu Dam is insufficient to moderate water quality degradation from agricultural runoff in the long term. Land use/cover change is an environmental problem that threatens the dam and social and economic crisis. Increasing population growth and land development contribute to land-use/cover changes. This results in severe deterioration of water quality in most freshwater bodies due to pollution and consequent eutrophication. This critical problem alarms water managers in terms of implementing a water quality system that considers other sectors. For example, data on the water quality can be developed if a well-defined link can be established between land use management and the water quality, both at the catchment and hydrological intensities.

Furthermore, for the sustainability of Mindu Dam, we suggest numerous policy effects to optimize the management. There is a need to develop a nexus of land-use/cover and water quality for monitoring, including preventing pollution. However, the success of such efforts will rely on coordinated actions by all stakeholders from different sectors. Therefore, mitigation and adaptation should be considered for water quality management of the dam, while land use management practices must be considered for sustainable resource management and water quality monitoring.

DATA AVAILABILITY STATEMENT

All relevant data are included in the paper or its Supplementary Information.

CONFLICT OF INTEREST

The authors declare there is no conflict.

REFERENCES

APHA 2012 Standard methods for the examination of water and wastewater. 22nd edition. Rice, E. W. & Bridgewater, L., American Public Health Association, American Water Works Association, Water Environment Federation, Washington DC.

Azyana, Y., Na, N. N. & Jannah, N. 2012 Land use and catchment size/scale on the water quality deterioration of Kinta River, Perak, Malaysia. *MJS* **31**(2), 121–131. https://doi.org/10.22452/mjs.vol31no2.4.

Chaudhry, F. & Malik, M. 2017 Factors affecting water pollution: a review. *Journal of Ecosystem & Ecography* **7**(225), 1–3. http://www.doi.org/10.4172/2157-7625.1000225.

Cheruto, M. C., Kauti, M. K., Kisangau, D. P. & Kariuki, P. C. 2016 Assessment of land use and land cover change using GIS and remote sensing techniques: a case study of Makueni County, Kenya. *Journal of Remote Sensing & GIS* **5** (4), 6.

Dube, T., Gumindoga, W. & Chawira, M. 2014 Detection of land cover changes around Lake Mutirikwi, Zimbabwe, based on traditional remote sensing image classification techniques. *African Journal of Aquatic Science* **39**(1), 89–95. http:/www.doi.org/10.2989/16085914.2013.870068.

Du Plessis, A., Harmse, T. & Ahmed, F. 2014 Quantifying and predicting the water quality associated with land cover change: a case study of the Blesbok Spruit Catchment, South Africa. *Water* **6**(10), 2946–2968. https://doi.org/10.3390/w6102946.

Guan, D., Li, H., Inohae, T., Su, W., Nagaie, T. & Hokao, K. 2011 Modeling urban land use change by the integration of cellular automaton and Markov model. *Ecological Modelling* **222**(20–22), 3761–3772.

Hassan, Z., Shabbir, R., Ahmad, S. S., Malik, A. H., Aziz, N., Butt, A. & Erum, S. 2016 Dynamics of land use and land cover change (LULCC) using geospatial techniques: a case study of Islamabad Pakistan. *SpringerPlus* **5**, 812. https://doi.org/10.1186/s40064-016-2414-z.

Kamusoko, C., Oono, K., Nakazawa, A., Wada, Y., Nakada, R., Hosokawa, T., Tomimura, S., Furuya, T., Iwata, A., Moriike, H., Someya, T., Yamase, T., Nasu, M., Gomi, Y., Sano, T., Isobe, T. & Homsysavath, K. 2011 Spatial simulation modelling of future forest cover change scenarios in Luangprabang province, Lao PDR. *Forests* **2**(3), 707–729.

Kashaigili, J. J. & Majaliwa, A. M. 2010 Integrated assessment of land use land cover changes in the Malagarasi river catchment in Tanzania. *Journal of Physics and Chemistry of the Earth* **35**, 730–741.

Kazi, T. G., Arain, M. B., Jamali, M. K., Jalbani, N., Afridi, H. I., Sarfraz, R. A., Baig, J. A. & Shah, A. Q. 2009 Assessment of water quality of polluted lake using multivariate statistical techniques: a case study. *Ecotoxicology and Environmental Safety* **72**(2), 301–309. https://doi.org/10.1016/j.ecoenv.2008.02.024.

Kibena, J., Nhapi, I. & Gumindoga, W. 2014 Assessing the relationship between water quality parameters and changes in landuse patterns in the Upper Manyame River, Zimbabwe. *Physics and Chemistry of the Earth, Parts A/B/C* **67–69**, 153–163. https://doi.org/10.1016/j.pce.2013.09.017.

Kumar, J., Biswas, B. & Walker, S. 2020 Multi-temporal LULC classification using hybrid approach and monitoring built-up growth with Shannon's entropy for a semi-arid region of Rajasthan, India. *Journal of the Geological Society of India* **95**(6), 626–635. https://doi.org/10.1007/s12594-020-1489-x.

Kumari, M., Das, A., Sharma, R. & Saikia, S. 2014 Change detection analysis using multi temporal satellite data of Poba reserve forest, Assam and Arunachal Pradesh. *International Journal of Geomatics and Geosciences* **4**(3), 517.

Lambin, E. F. 1997 Modelling and monitoring land-cover change processes in tropical regions. *Progress in Physical Geography: Earth and Environment* **21**(3), 375–393. https://doi.org/10.1177/030913339702100303.

Li, H., Reynolds, J. F., 1997 Modeling effects of spatial pattern, drought, and grazing on rates of rangeland degradation: a combined Markov and cellular automaton approach. In: *Scale in Remote Sensing and GIS* (Quattrochi, D. A. & Goodchild, M. F., eds). Lewis Publishers, New York, pp. 211–230.

Li, C., Wang, J., Wang, L., Hu, L. & Gong, P. 2014 Comparison of classification algorithms and training sample sizes in urban land classification with landsat thematic mapper imagery. *Remote Sensing* **6**(2), 964–983. https://doi.org/10.3390/rs6020964.

Mdegela, R. H., Braathen, M., Pereka, A. E., Mosha, R. D., Sandvik, M. & Skaare, J. U. 2009 Heavy metals and organochlorine residues in water, sediments, and fish in aquatic ecosystems in urban and peri-urban areas in Tanzania. *Water, Air, and Soil Pollution* **203**(1), 369–379. https://doi.org/10.1007/s11270-009-0019-7.

Mdegela, R. H., Mosha, R. D., Ngowi, H. A. & Nonga, H. 2013 Environmental and health impacts associated with usage of agrochemicals in Mindu dam catchment area, Morogoro, Tanzania. *Huria: Journal of the Open University of Tanzania* **15**(1), 18–33.

Myint, S. W. & Wang, L. 2006 Multicriteria decision approach for land use land cover change using Markov chain analysis and a cellular automata approach. *Canadian Journal of Remote Sensing* **32**(6), 390–404.

Mzuza, M. K., Zhang, W., Kapute, F. & Wei, X. 2019 *The Impact of Land Use and Land Cover Changes on the Nkula Dam in the Middle Shire River Catchment, Malawi Geospatial Analyses of Earth Observation (EO) Data*. IntechOpen.

Namugize, J. N., Jewitt, G. & Graham, M. 2018 Effects of land use and land cover changes on water quality in the uMngeni river catchment, South Africa. *Physics and Chemistry of the Earth, Parts A/B/C* **105**, 247–264. https://doi.org/10.1016/j.pce.2018.03.013.

Natkhin, M., Dietrich, O., Schäfer, M. P. & Lischeid, G. 2015 The effects of climate and changing land use on the discharge regime of a small catchment in Tanzania. *Regional Environmental Change* **15**(7), 1269–1280. https://doi.org/10.1007/s10113-013-0462-2.

Ngonyani, C. J. & Nkotagu Hudson, H. 2007 Study of nutrient pollutants and their impacts on the water quality of the Mindu reservoir at Morogoro municipality. *Tanzania Journal of Engineering and Technology* **1**(3), 138–148. http://www.doi.org/10.10520/AJA1821536X_38.

Palinkas, L. A., Horwitz, S. M., Green, C. A., Wisdom, J. P., Duan, N. & Hoagwood, K. 2015 Purposeful sampling for qualitative data collection and analysis in mixed method implementation research. *Administration and Policy in Mental Health and Mental Health Services Research* **42**(5), 533–544. https://doi.org/10.1007/s10488-013-0528-y.

Panwar, S. & Malik, D. 2017 Evaluating land use/land cover change dynamics in Bhimtal lake catchment area, using remote sensing & GIS techniques. *Journal of Remote Sensing and GIS* **6**(199), 2. http://www.doi.org/10.4172/2469-4134.1000199.

Rajib, M. A., Ahiablame, L. & Paul, M. 2016 Modeling the effects of future land use change on water quality under multiple scenarios: a case study of low-input agriculture with hay/pasture production. *Sustainability of Water Quality and Ecology* **8**, 50–66. https://doi.org/10.1016/j.swaqe.2016.09.001.

Ramadas, M., Samantaray, A. K., 2018 Applications of remote sensing and gis in water quality monitoring and remediation: a state-of-the-art review. In: *Water Remediation* (Bhattacharya, S., Gupta, A. B., Gupta, A. & Pandey, A., eds). Springer Singapore, Singapore, pp. 225–246.

Ranjan, R. K. & Kumari, P. 2018 Impact of land use and land cover changes on nutrients concentration in and around Kabartal wetland, Begusarai (Bihar), India. In: Chander Kumar Singh (ed.), *Geosptaial Applications for Natural Resource Management*, Boca Raton, CRC Press, pp. 243–250.

Riccioli, F., El Asmar, T., El Asmar, J. P. & Fratini, R. 2013 Use of cellular automata in the study of variables involved in land use changes: an application in the wine production sector. *Environmental Monitoring and Assessment* **185**, 5361–5374.

Roose, M. & Hietala, R. 2018 A methodological Markov-CA projection of the greening agricultural landscape – a case study from 2005 to 2017 in southwestern Finland. *Environmental Monitoring and Assessment* **190**, 1–13.

Rozario, P. & Gomes, R. 2021 Comparison of data mining algorithms in remote sensing using Lidar data fusion and feature selection. In: *2021 IEEE International Conference on Electro Information Technology (EIT)*, pp. 236–243. https://doi.org/10.1109/EIT51626.2021.9491878.

Sagan, V., Peterson, K. T., Maimaitijiang, M., Sidike, P., Sloan, J., Greeling, B. A., Maalouf, S. & Adams, C. 2020 Monitoring inland water quality using remote sensing: potential and limitations of spectral indices, bio-optical simulations, machine learning, and cloud computing. *Earth-Science Reviews* **205** (August 2019), 103187. https://doi.org/10.1016/j.earscirev.2020.103187.

Subedi, P., Subedi, K. & Thapa, B. 2013 Application of a hybrid cellular automaton–Markov (CA-Markov) model in land-use change prediction: a case study of Saddle Creek Drainage Basin, Florida. *Applied Ecology and Environmental Sciences* **1**(6), 126–132.

Sun, J., Yang, J., Zhang, C., Yun, W. & Qu, J. 2013 Automatic remotely sensed image classification in a grid environment based on the maximum likelihood method. *Mathematical and Computer Modelling* **58**(3–4), 573–581. https://doi.org/10.1016/j.mcm.2011.10.063.

Tahiru, A. A., Doke, D. A. & Baatuuwie, B. N. 2020 Effect of land use and land cover changes on water quality in the Nawuni Catchment of the White Volta Basin, Northern Region, Ghana. *Applied Water Science* **10**(8), 1–14. https://doi.org/10.1007/s13201-020-01272-6.

Teixeira, Z., Teixeira, H. & Marques, J. C. 2014 Systematic processes of land use/land cover change to identify relevant driving forces: implications on water quality. *Science of The Total Environment* **470–471**, 1320–1335. https://doi.org/10.1016/j.scitotenv.2013.10.098.

Twisa, S. & Buchroithner, M. F. 2019 Land-use and land-cover (LULC) change detection in Wami River Basin, Tanzania. *Land* **8**(9), 136.

Vitousek, P. M., Naylor, R., Crews, T., David, M. B., Drinkwater, L. E., Holland, E., Johnes, P. J., Katzenberger, J., Martinelli, L. A., Matson, P. A., Nziguheba, G., Ojima, D., Palm, C. A., Robertson, G. P., Sanchez, P. A., Townsend, A. R. & Zhang, F. S. 2009 Nutrient imbalances in agricultural development. *Science* **324**(5934), 1519. http://www.doi.org/10.1126/science.1170261.

Yang, H., Kong, J., Hu, H., Du, Y., Gao, M. & Chen, F. 2022 A review of remote sensing for water quality retrieval: progress and challenges. *Remote Sensing* **14**(8). https://doi.org/10.3390/rs14081770

First received 7 November 2022; accepted in revised form 15 April 2023. Available online 28 April 2023